

Doubly Uniparental Inheritance of Mitochondria As a Model System for Studying Germ Line Formation

Liliana Milani*, Fabrizio Ghiselli, Maria Gabriella Maurizii, Marco Passamonti

Department of Biologia Evoluzionistica Sperimentale, University of Bologna, Bologna, Italy

Abstract

Background: Doubly Uniparental Inheritance (DUI) of mitochondria occurs when both mothers and fathers are capable of transmitting mitochondria to their offspring, in contrast to the typical Strictly Maternal Inheritance (SMI). DUI was found in some bivalve molluscs, in which two mitochondrial genomes are inherited, one through eggs, the other through sperm. During male embryo development, spermatozoon mitochondria aggregate in proximity of the first cleavage furrow and end up in the primordial germ cells, while they are dispersed in female embryos.

Methodology/Principal Findings: We used MitoTracker, microtubule staining and transmission electron microscopy to examine the mechanisms of this unusual distribution of sperm mitochondria in the DUI species *Ruditapes philippinarum*. Our results suggest that in male embryos the midbody deriving from the mitotic spindle of the first division concurs in positioning the aggregate of sperm mitochondria. Furthermore, an immunocytochemical analysis showed that the germ line determinant Vasa segregates close to the first cleavage furrow.

Conclusions/Significance: In DUI male embryos, spermatozoon mitochondria aggregate in a stable area on the animal-vegetal axis: in organisms with spiral segmentation this zone is not involved in cleavage, so the aggregation is maintained. Moreover, sperm mitochondria reach the same embryonic area in which also germ plasm is transferred. In 2-blastomere embryos, the segregation of sperm mitochondria in the same region with Vasa suggests their contribution in male germ line formation. In DUI male embryos, M-type mitochondria must be recognized by egg factors to be actively transferred in the germ line, where they become dominant replacing the Balbiani body mitochondria. The typical features of germ line assembly point to a common biological mechanism shared by DUI and SMI organisms. Although the molecular dynamics of the segregation of sperm mitochondria in DUI species are unknown, they could be a variation of the mechanism regulating the mitochondrial bottleneck in all metazoans.

Citation: Milani L, Ghiselli F, Maurizii MG, Passamonti M (2011) Doubly Uniparental Inheritance of Mitochondria As a Model System for Studying Germ Line Formation. PLoS ONE 6(11): e28194. doi:10.1371/journal.pone.0028194

Editor: David E. Clapham, Harvard Medical School, United States of America

Received: July 12, 2011; **Accepted:** November 2, 2011; **Published:** November 29, 2011

Copyright: © 2011 Milani et al. This is an open-access article distributed under the terms of the Creative Commons Attribution License, which permits unrestricted use, distribution, and reproduction in any medium, provided the original author and source are credited.

Funding: This work was supported by the University and Research Italian Ministry (MIUR PRIN07, grant number 2007NSHJL8_002 to MP) and the "Canziani Bequest" fund (University of Bologna, grant number A.31.CANZELSEW to MP). The funders had no role in study design, data collection and analysis, decision to publish, or preparation of the manuscript.

Competing Interests: The authors have declared that no competing interests exist.

* E-mail: liliana.milani@unibo.it

Introduction

The origin of Primordial Germ Cells (PGCs) is a central issue in developmental biology. In many animals, cells that inherit the germ plasm during the first embryonic divisions give rise to PGCs [1–8]. The germ plasm is a specific part of the egg cytoplasm, whose composition is similar in widely divergent phyla: it mainly contains proteins from conserved germ cell-specific genes and RNAs, mRNAs and non-coding RNAs, used for translation when post-transcriptional processing reactivates after fertilization [9–11]. A typical component of germ plasm is the DEAD-box RNA helicase Vasa, firstly characterized in *Drosophila melanogaster* [12,13], and then isolated in many invertebrates and vertebrates [14]. Inactivation of this helicase suppresses the formation of PGCs [15–18]. Interestingly, the aggregation of *vasa* products in the germ plasm appears to occur either at protein or transcript level, depending on the organism [19]. Germ plasm can be identified with Transmission Electron Microscopy (TEM) by the presence of electron-dense granulofibrillar material which is called "nuage",

often positioned near the nucleus and associated with mitochondria [7,10,20]. The nuage stores RNAs and proteins that are produced early in oogenesis and, in oocytes, it associates with a distinctive structure known as Balbiani Body (Bb), which includes also a mitochondrial mass and Golgi complexes [7,10,21]. Subsequently, the Bb is transported in the cytoplasm area of the egg that, after fertilization, is taken up by PGCs [10]. In male germinal cells, the nuage is called chromatoid body (Cb), and is typically associated with mitochondria [22,23]. The Cb is first clearly seen in mid- and late pachytene spermatocytes as an inter-mitochondrial dense material [23]. Then, during spermiogenesis, the Cb acquires a lobular structure and is surrounded by a multitude of vesicles, near the Golgi complex, and frequently connected by material continuities with the nucleus through nuclear pores [23–25]. Later in spermiogenesis, at least in mammals, the Cb takes part in the formation of the residual body, a ring adjacent to the midpiece [23,26].

The frequent colocalization of mitochondria and nuage suggests a connection between these organelles and germ line development.

For example, mitochondrial ribosomes are found extramitochondrially and are required to produce proteins necessary for germ cell formation [4,27–32]. Moreover, evidence from TEM analysis documented the extrusion of material and cristae from mitochondria forming nuage both in gametes during gametogenesis [20,33] and in developing embryos [20,32,34]. Actually, in early embryos a mitochondrial-type translation is required for germ cell formation, which is disrupted by the injection of prokaryotic translation inhibitors [35]. Another supporting clue to a role of mitochondria in germ line formation comes from their origin: they have a common ancestor with the endosymbiont Rickettsiales [36], some of which are known to distort the sex of their host. *Wolbachia*, for example, induces male killing, feminization, parthenogenesis, cytoplasmic incompatibility [37,38], and methylation pattern modification in gonads [39]. Accordingly, depletion of mtDNA results in significant changes in the methylation pattern of a number of nuclear genes, some of which are reversed by the restoration of mtDNA [40].

Another fundamental question in developmental biology is which mitochondria effectively enter the germ line. A bottleneck has been proposed based on the observation that mitochondrial genomes in each individual are largely homoplasmic, despite their high mutation rate [41–43]. In oocytes of many organisms two populations of mitochondria can be distinguished: one population is aggregated in the Bb and enters the embryo PGCs during development [7,21,34], while the remaining mitochondria spread in the oocyte and are transmitted to the somatic lineage [44–46]. For this reason, the Bb mitochondrial population or a part of it may actually represent the mitochondrial bottleneck [47]. Since all mitochondria are usually transmitted to embryos through oocytes, the bottleneck is generally believed to be under female control, but factors from spermatozoon might also be involved in mitochondrial inheritance and selection [48]. The process by which mitochondria enter the developing germ line is still unknown, but the involvement of microtubules in their general distribution was confirmed by experiments using inhibitors to microtubule polymerization [49–51].

To address the relationship between mitochondria and germ line formation we study an unusual system of mitochondrial transmission known as Doubly Uniparental Inheritance (DUI) (reviewed in [52,53]). Commonly, metazoan mitochondria experience Strictly Maternal Inheritance (SMI), i.e. they are transmitted by females only, because mitochondria from spermatozoon are excluded or degraded [54–57]. The only known exception comes from some bivalve molluscs ([58] and references therein), in which two mitochondrial lineages are inherited, one through eggs (F-type), the other through sperm (M-type), and showing up to 52% sequence divergence [59]. In DUI male embryos, spermatozoon mitochondria form an aggregate [49,60–62], and, during development, this aggregate enters PGCs, as proved by the specific presence of M-type mtDNA in spermatozoa [63,64]. In DUI female embryos sperm mitochondria are dispersed and the mitochondrial inheritance would be as in SMI species [49,60,61,64–66]. Moreover, in DUI *Mytilus* species sex-ratio distortion was observed: females were found producing a female-biased offspring and showing a majority of dispersed patterns, other females produced a male-biased progeny with a majority of aggregated patterns, and others a 50:50 sex-ratio, with a balanced frequency of the two patterns [61,65,67]. Recently, sex-ratio biased progenies were also found in the DUI species *Ruditapes philippinarum* Adams & Reeve [68]. The peculiar segregation pattern of spermatozoon mitochondria, correlated with the existence of sex-biased lineages, led to the hypothesis that M-type mitochondria could have an active role in the masculinization of

the gonad, achieved through a series of specific signals between the nucleus and mitochondria [67].

The Manila clam *R. philippinarum* belongs to the family Veneridae, it is strictly gonochoric and its gonad forms every year at the beginning of the mating season, after which it is degraded [69]. During the non-reproductive season sex cannot be determined [69]. Like other protostomes, molluscs follow a spiralian embryonic development: embryo blastomeres receive a

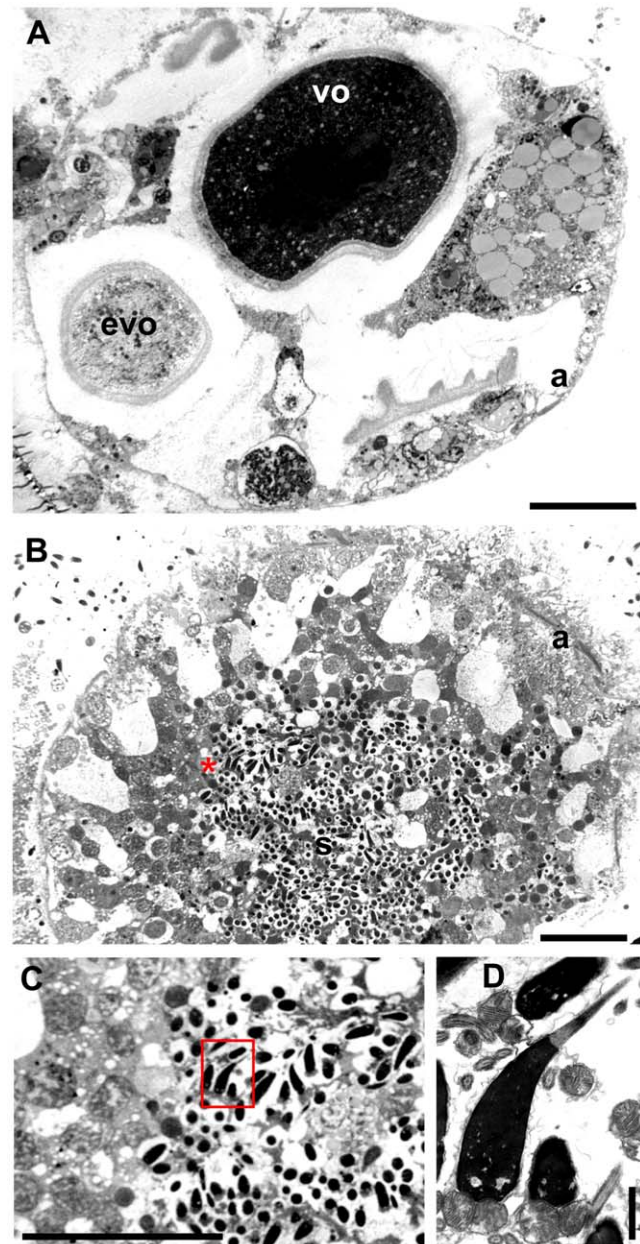


Figure 1. Morphological analysis of female and male gonads in *R. philippinarum* (TEM). (A) A female acinus, with oocytes at different stages of differentiation; evo – early vitellogenic oocyte; vo – vitellogenic oocyte; a – acinus wall (20 μ m bar). (B) Portion of a male acinus in which spermatogenesis is developing centripetally, with mature spermatozoa (s) free within the acinus lumen (20 μ m bar). (C) Magnification, from B, of the detail at the right side of the red asterisk, showing mature spermatozoa (20 μ m bar). (D) The detail squared in C: a sperm head with acrosome and mitochondrial midpiece (1 μ m bar). doi:10.1371/journal.pone.0028194.g001

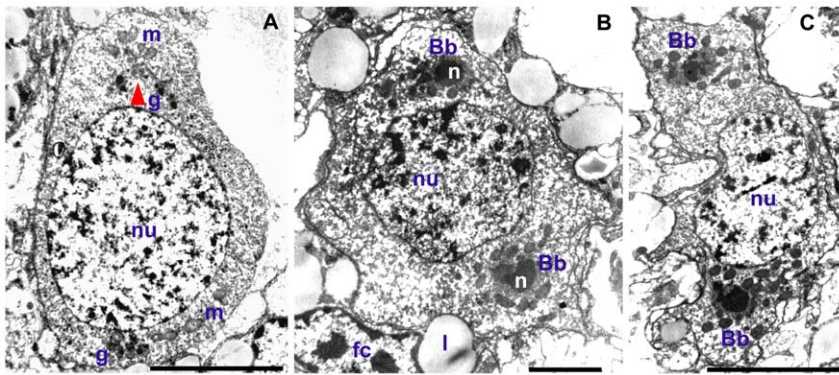


Figure 2. Ultrastructural analysis of the Balbiani body formation in *R. philippinarum* (TEM). (A) Oogonium showing electron-dense granules (g) close to two mitochondrial masses (m) at opposite sides of the nucleus (nu) (5 μ m bar). (B, C) In early oocytes two identical Balbiani bodies (Bbs) are present, both containing a large and dense nuage (n) and a mitochondrial mass. fc – follicle cell; l – lipid droplet (B: 2 μ m bar; C: 5 μ m bar). doi:10.1371/journal.pone.0028194.g002

specific content of cytoplasm, and they can be tracked through development up to the formation of organs [70]. PGCs arise from the 4d mesentoblast formed during the sixth cell division ([70] and references therein), but the mechanisms of sexual differentiation of the gonad are still unknown.

Exploiting the peculiar features of DUI, we investigated the specific segregation of spermatozoon mitochondria in clam embryos. Although the molecular dynamics of their segregation is still largely unknown, it could be a variation of the mechanism that regulates the mitochondrial bottleneck in all metazoans. In *R. philippinarum*, we found a series of typical structures related to germ line formation, pointing to a common biological mechanism shared by DUI and SMI organisms. All that considered, DUI can certainly provide important information on mitochondrial inheritance dynamics and functions.

Methods

Spawning induction and fertilization

R. philippinarum clams used in mating experiments were collected in Goro (Italy) during the reproductive season (July/August). The spawning was induced with cycles of cold and warm artificial sea water (e.g. reverse osmosis water added with RedSea Coral Pro aquarium sea salt, at 22 and 29°C) every 30 min. After fertilization, embryo development was visually checked with an optical microscope. Samples of 2-, 4-, 8-blastomere embryos were collected. Clams for gonad analysis were sampled in February (developing), and in May (mature).

MitoTracker staining

The vital mitochondrial dye MitoTracker Green FM (Molecular Probes), dissolved in anhydrous dimethylsulfoxide (DMSO) (Sigma), was added to the sperm suspension at 200 nM of final concentration. The sperm was incubated for 20 minutes at room temperature (RT) in the dark and then used in small amount to fertilize eggs. The embryos were put on slides coated with 3-aminopropyltriethoxysilane (APES; Sigma) and mounted directly in sea water. The visualization was performed by a Nikon Eclipse 90i fluorescence microscope using a FITC filter and pictures were recorded by NIS-elements AR 3.0 software.

Transmission Electron Microscopy (TEM)

Sample preparation for TEM analysis was performed as follows: gonadic tissue was dissected with a scalpel and immediately fixed

for 2 hours in glutaraldehyde 2%, then rinsed in salt water and post-fixed in 1% osmium tetroxide in salt water for 1 h. After rinsing in salt water, we proceeded with dehydration with increasing concentrations of acetone (50–100; 70% acetone solution contained 1% uranyl acetate). Samples were then embedded in resin (Fluka Durcupan ACM). Polymerization was completed after 3–4 days at 60°C, followed by 1–2 days at 45°C. A

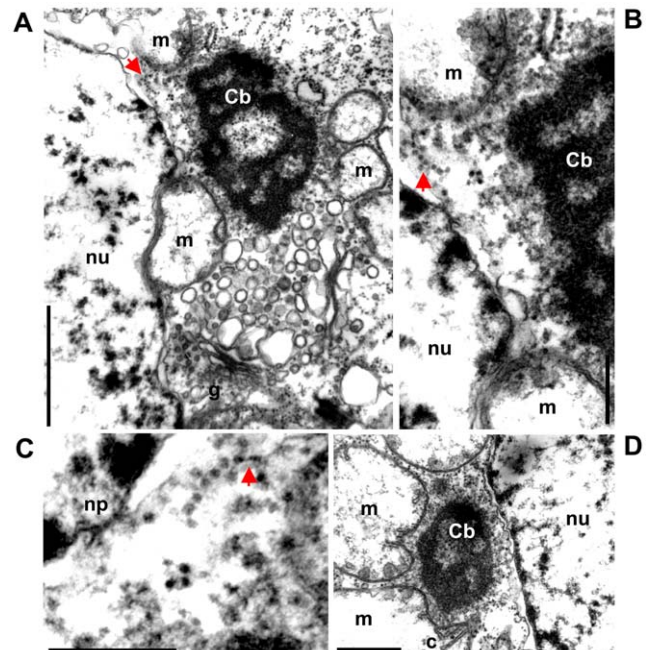


Figure 3. Ultrastructural analysis of the Chromatoid body formation in *R. philippinarum* (TEM). (A) Cytoplasmic area around the Chromatoid body (Cb) in an early spermatid (1 μ m bar); nu – nucleus; g – Golgi apparatus. (B) A detail from A showing the region among nucleus, mitochondria (m) and the Cb (250 nm bar). (C) A detail of B: nuclear material outflows from a nuclear pore (np) and a polyribosome formed by ribosomes of two different sizes is visible, the smallest are indicated by an arrow (250 nm bar). (D) The Cb is located close to the nuclear membrane and surrounded by empty mitochondria, some of which showing extruded cristae (c) (500 nm bar). arrow – polyribosome. doi:10.1371/journal.pone.0028194.g003

Reichert ultramicrotome was used to cut silver-gold ultrathin sections (60–90 nm) using diamond knives. Ultrathin sections were collected on 75 mesh, copper grids coated by formvar and then stained with 3% uranyl acetate and with lead citrate. Sections were examined using a Philips CM100 (PW6021) TEM at 80 kV. Pictures were recorded with a Kodak MEGAPLUS Camera, Model 1.6i, using AnalySIS® Software.

SDS-PAGE and western blotting

Pieces of gonads and embryos were frozen in liquid nitrogen, stored at -80°C , and then processed by SDS-PAGE (Sodium Dodecyl Sulphate - PolyAcrylamide Gel Electrophoresis) and western blotting. Embryos of 2, 4 and 8 blastomeres were pooled for this analysis. Samples were homogenized in a buffer containing 10 mM Tris-HCl, pH 7.5, 1 mM ethylene glycol-bis(2-aminoethyl ether)-N,N,N',N'-tetraacetic acid (EGTA), 0.1% SDS in the presence of 2x protease inhibitor cocktail tablets (Complete Mini, Roche) and 1 mM PMSF, utilizing an Ultra Turrax T25 Janke & Kunkel IKA-laborstechnik. Then samples were centrifuged at 10,000 rpm for 10 minutes at 4°C . The supernatant was stored at -80°C . Gonadic and embryonic extracts of *R. philippinarum* (10 μg) were separated in 8.5% SDS polyacrylamide gels according to Laemmli [71]. For immunoblotting, proteins were transferred to Hybond-ECL membrane (Amersham International, Buckinghamshire, UK). Non-specific protein-binding sites were blocked with 5% dried skimmed milk (Bio-Rad Laboratories, Hercules, CA, USA), 3% Bovine Serum Albumin (BSA), and 0.1% Tween-20 (Sigma) in TBS overnight at 4°C and subsequently washed with 0.1% Tween TBS. To recognize Vasa protein, we utilized an antiserum against chicken Vasa-homolog produced in rabbit already in use in our laboratory (anti-Cvh; [72]). The membranes were treated as described in Maurizii et al. [73]. A bidimensional SDS-PAGE of gonadic extract was carried out as in GE Healthcare Handbook (80-6429-60AC).

vasa-homolog

We analyzed the *vasa*-like gene of *R. philippinarum* found by whole transcriptome sequencing of gonads [68]. An ORF of 2,373 bp was identified, translated and aligned with Cvh (*Gallus gallus*, GenBank BAB12337.1) using T-COFFEE, version 8.99 [74]. Conserved domains were identified using InterProScan, version 4.8 [75].

Tissue processing and immunocytochemical analyses

Embryos. Embryos were fixed in a solution containing 3.7% paraformaldehyde, 0.1% glutaraldehyde, and 1.5 μM taxol in K-PIPES buffer [80 mM K Pipes; 1 mM MgCl_2 ; 5 mM EGTA; 0.2% Triton X-100] (pH 6.8) for 30 minutes at 37°C . After several washes in Tris-Buffered Saline solution [TBS: 155 mM NaCl; 10 mM Tris-HCl] (pH 7.4), embryos were put in methanol and stored at 4°C . After rehydration with TBS (pH 7.4), fixed embryos were put on slides coated with APES (Sigma), treated with 50 mM sodium borohydride in TBS for 60 minutes at RT and rinsed in TBS with several changes. Embryos for microtubule staining were digested with 0.01% Pronase E (Merck) in Phosphate-Buffered Saline solution (PBS) [128 mM NaCl; 2 mM KCl; 8 mM $\text{Na}_2\text{HPO}_4 \cdot 2\text{H}_2\text{O}$; 2 mM KH_2PO_4] (pH 7.2), for 6–7 minutes at RT. Permeabilization was performed adding TBS-Triton 1% to all the samples and leaving over night at 4°C .

Vasa immunostaining. Non-specific protein-binding sites were blocked with a buffer containing 10% Normal Goat Serum (NGS) and 1% BSA in TBS 0.1% Triton (pH 7.4). The primary antibody (anti-Cvh) was diluted 1: 2,000 with TBS containing 0.1% Triton, 10% Normal Goat Serum (NGS), and 1% BSA (pH 7.4) for 48 hours at 4°C . As secondary antibody we employed a goat anti-rabbit polyclonal antibody, conjugated with N,N'-dipropyl-tetramethylindocarbocyanine (Cy3) (Zymed, Molecular Probes), diluted 1: 300 with TBS containing 0.1% Triton, 10% NGS, and 1% BSA (pH 7.4) for 30 hours at 4°C .

Microtubule immunostaining. Embryos were incubated with a monoclonal anti- α -tubulin, clone DM 1A (Sigma), diluted 1: 1,800 with TBS-Triton 0.1% and 2% BSA (pH 7.4) for 48 hours at 4°C . Bound primary antibody was detected using Cy3-conjugate anti-mouse, produced in sheep (Sigma), diluted 1: 300 with TBS-Triton 0.1%, 2% BSA (pH 7.4), with about 40 hours of incubation at 4°C .

Nuclei of all samples were stained with 1 mM TO-PRO3 (Molecular Probes) diluted 1: 2,000 in PBS (pH 7.2) at RT. Samples were mounted in 2.5% 1,4-diazabicyclo[2.2.2]octane (DABCO; Sigma), 50 mM Tris (pH 8) and 90% glycerol, and stored at 4°C .

Controls were performed using embryos in which the first or the second antibody was omitted, and embryos treated only with normal serum. Imaging of embryos was recorded by a confocal laser scanning microscope (Leica confocal SP2 microscope), using Leica software.

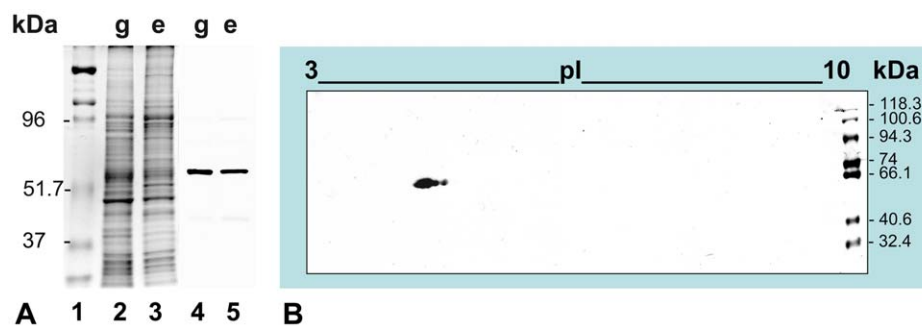


Figure 4. Specificity of the anti-Cvh antibody. (A) Monodimensional electrophoresis and immunoblotting of gonadic and embryonic extracts of *R. philippinarum*. Gel Coomassie stained (lanes 1–3). Lane 1: molecular mass standards with the value in kilodaltons (kDa) on the left. Lane 2: gonadic extract (g). Lane 3: embryonic extract (e). The antiserum against chicken Vasa-homolog (anti-Cvh) marks one protein band of about 65 kDa, both in gonadic and embryonic extracts (lanes 4, 5). (B) Bidimensional immunoblotting of gonadic extract with anti-Cvh. The antibody detects one big spot flanked by two smaller, all of about 65 kDa as molecular mass and with isoelectric point (pI) around 5. doi:10.1371/journal.pone.0028194.g004

D). Four mitochondria of about 1 μm in diameter form the midpiece of *R. philippinarum* spermatozoon, while egg mitochondria are quite smaller (about 0.6 μm in vitellogenic oocytes) [62]. The ultrastructural analysis of developing gametes allowed the identification of both Balbiani body (Bb, Figure 2) and Chromatoid body (Cb, Figure 3), in early oocytes and early spermatids, respectively. Oogonia showed electrondense granules aggregating near two mitochondrial masses at opposite sides of the nucleus (Figure 2A), where in early oocytes they formed the nuage of two identical Bbs (Figure 2B and C). Each Bb was characterized by a dense nuage of about 1 μm and a mitochondrial mass of 10–28 organelles per section (Figure 2B and C). In early spermatids the ultrastructural analysis allowed the identification of a typical Chromatoid body (Cb) (Figure 3), a bit longer than 1 μm , always located close to the nuclear membrane and surrounded by empty mitochondria (Figure 3). A pore in the nuclear membrane could be seen emitting material near the Cb (Figure 3A–C). In the area among the nuclear pore, the empty mitochondria and the Cb, ribosomes of two different sizes were found on polyribosomes, with the small ones localized in a restricted zone (Figure 3B and C).

R. philippinarum vasa-homolog

The specificity of the anti-vasa Chicken antibody (anti-Cvh) was tested by performing mono and bidimensional western blot. In both gonad and embryo samples, monodimensional immunoblotting with anti-Cvh detected only one band of about 65 kDa as molecular mass (Figure 4A). In gonadic extract, the bidimensional analysis showed one big spot flanked by two smaller, all of about 65 kDa and isoelectric point (pI) around 5 (Figure 4B). We also analyzed the vasa homolog of *R. philippinarum* found by whole transcriptome sequencing of gonads [68]. We named it *vasph* (*vasa philippinarum* homolog). The inferred aminoacid sequence included 790 residues. The T-COFFEE protein alignment with the chicken Vasa-homolog showed a good CORE index (score = 95) [76] (Figure 5). Using InterProScan, four CCHC-type zinc fingers (GO:0008270, location: 176–192; 204–220; 231–247; 259–275), a DEAD-box RNA helicase (GO:0008026, location: 361–540), and a C-terminal helicase (GO:0004386, location: 607–683) were found (Figure 6). In addition, in the predicted protein sequence five RNA-binding RGG motifs were included in the N-terminal region (Figure 6).

Once verified the specificity of anti-Cvh, we analyzed Vasph expression in gonads and in early embryos of *R. philippinarum*. At the beginning of the reproductive season, when gonads start forming, we found that anti-Cvh labeled small groups of cells

(Figure 7A and B). These Vasph-stained cells were detected in the connective tissue among unlabeled intestinal loops (Figure 7A), which is the normal position of bivalve gonad formation [69]. In a following stage of gonad differentiation, Vasph-labeled cells formed an empty space in the middle of the aggregate, becoming the wall of incipient acini with a lumen at the center (Figure 7C–F). Finally, in mature gonads acini appeared full of gametes (Figure 7G–H). In a female acinus (Figure 7G), oocytes showed a diffused cytoplasmic immunolocalization of Vasph. A small aggregation of granules was evident in the cytoplasm of the biggest oocyte (Figure 7G). In male acini, a diffused staining was found in spermatogenic cells along the acinus wall (Figure 7H). In spawned eggs, Vasph-staining showed granules dispersed in the cytoplasm, with no evident pattern of aggregation (Figure 8A). On the contrary, in 2-blastomere embryos Vasph immunostaining showed a more strongly stained zone along the cleavage furrow, both with confocal (Figure 8B) and fluorescence (Figure 8C) microscope. Some bigger labeled spots were aggregated where the midbody formed (Figure 8B–E). Control embryos did not show any labeling (Figure 8F).

Distribution of microtubules and spermatozoon mitochondria in early embryos

Microtubule staining with anti- α -tubulin antibody in early embryos showed a higher density of short microtubules along the blastomere cortex and longer microtubules between cortex and nuclei, underlining the structural function of microtubular cytoskeleton in positioning the nucleus at the center of the cell (Figure 9). Furthermore, microtubule staining showed a well-defined midbody located in the middle of the cleavage furrow of 2-blastomere embryos (Figure 9D and E). In the same area the four mitochondria from spermatozoon were aggregated in male embryos, as shown by MitoTracker staining (Figure 9A; see also [62]). In 4-blastomere embryos the new spindles (marked by the two midbodies in Figure 9F and G) formed in tangential directions, around the region where the four M-type mitochondria were located, that was on the animal-vegetal (a–v) axis (Figure 9B, and scheme in Figure 10). The same could be seen in 8-blastomere embryos (Figure 9C and H).

Finally, in some 2-blastomere embryos, TEM observations clearly showed a midbody associated to mitochondria of about 1 μm (Figure 11), which were most likely the M ones. Moreover, in some sections, a centriole appeared to still link spermatozoon mitochondria (Figure 11B). At the cleavage level, there was always

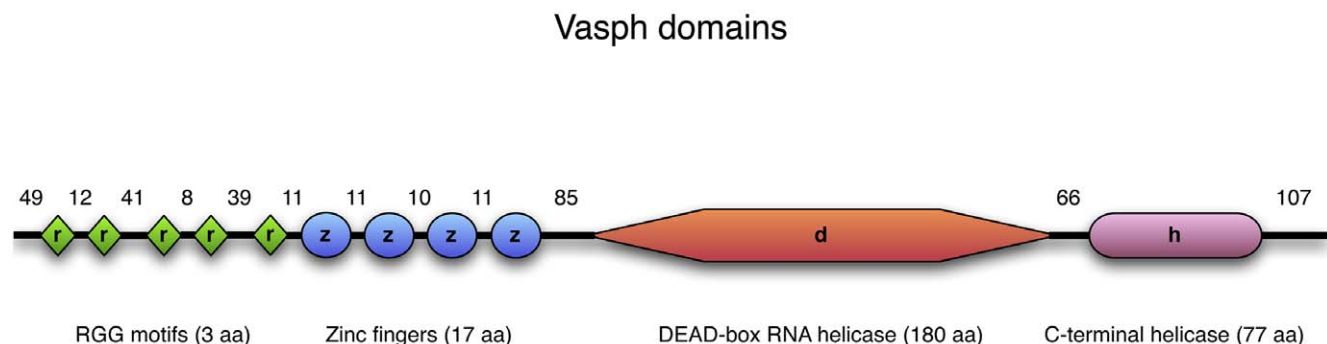


Figure 6. Vasph domains. Vasa conserved domains found in Vasph inferred sequence by InterProScan (version 4.8). There are four CCHC-type zinc fingers (17 aminoacids, aa, each), a DEAD-box RNA helicase (180 aa), and a C-terminal helicase (77 aa). In addition, five RNA-binding RGG motifs are included in the N-terminal region. The number of aminoacids of the regions between the domains are reported above the scheme. doi:10.1371/journal.pone.0028194.g006

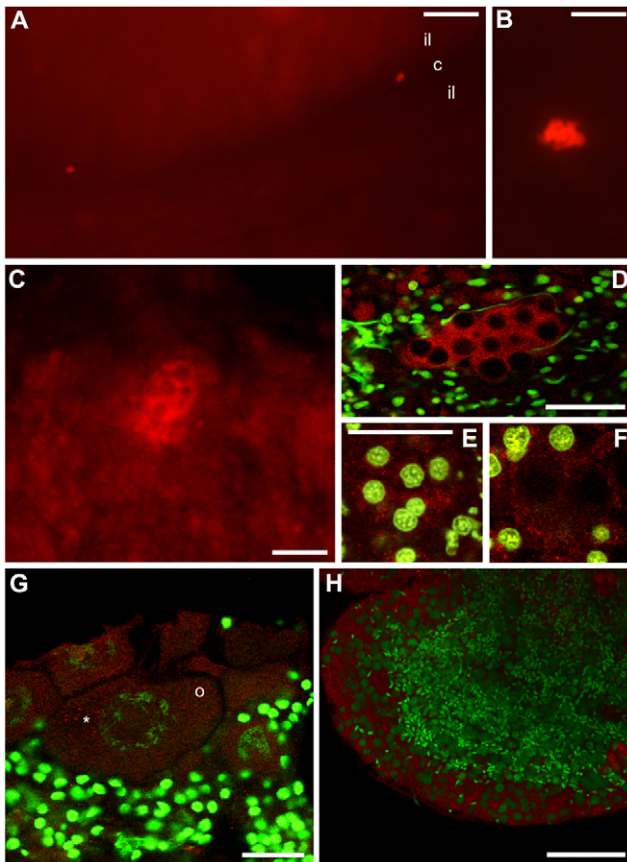


Figure 7. Vasph immunolocalization with anti-Cvh during *R. philippinarum* gonad differentiation. (A–C) Fluorescence microscope analysis on sections of a gonad at the beginning of its differentiation. (A) Two small spots result labeled in the connective tissue (c) between two intestinal loops (il), that are not labeled (250 μ m bar). (B) In a magnification of A the staining of the early gonad is better visible (50 μ m bar). (C) A following stage of gonadic development, in which the germ cells, strongly stained, start forming acini with some big cavities in the middle (50 μ m bar). (D–F) Confocal analysis on sections of a more differentiated gonad. Anti-Cvh (red) and TO-PRO-3 iodide staining DNA (green). (D) Incipient acini with some Vasph stained cells visible on a line around the cavities; the numerous cells of the surrounding connective tissue are not labeled (50 μ m bar). (E, F) Two images at various depths, within the same sample of D. (E) Germ cells with big nuclei and a strong Vasph-staining are visible (24 μ m bar). (F) In a deeper region of the gonadic tissue observed in E, the labeled germ cells are located around a still empty acinus lumen (same magnification of E). (G, H) Confocal analysis on sections of female and male mature gonads. (G) Oocytes strictly packed in an elongated acinus show a diffuse cytoplasmic immunolocalization of Vasph. In the biggest oocyte (o), some strongly labeled granules are seen in a region of the cytoplasm (asterisk) (30 μ m bar). (H) Male acinus full of spermatozoa: a diffused staining is present only in the spermatogenic cells located near the acinus wall (50 μ m bar).
doi:10.1371/journal.pone.0028194.g007

an abundance of F-type mitochondria, clearly recognizable by their smaller size, some of which fusing with the cleavage membrane (Figure 11B).

Discussion

Unusual and conserved features of germ cells in DUI organisms

Germ line formation is a central topic to understand development. Recent researches [32–35] indicate that mitochon-

dria play a key role in several steps of this process. For this reason, we used a DUI experimental system whose features provide a unique point of view for understanding the influence of mitochondria on germ line development, and we searched for typical structures involved in germ line specification. In *R. philippinarum* oogonia, TEM analysis showed electron-dense granules that aggregate close to two mitochondrial masses at the opposite sides of the nucleus (Figure 2A). In oocytes these structures form two identical Bbs (Figure 2B and C) similar to those described in other animals. The presence of two distinct Bbs is an unusual feature; actually, as far as we know, *R. philippinarum* is the first species showing two Bbs in each oocyte, both containing a nuage clearly recognizable with TEM. This feature might be tentatively interpreted as a remnant of an archaic hermaphroditic condition [77]. In fact, hermaphrodite bivalves present an ovotestis with two separated parts: one producing eggs, the other producing sperm. Moreover, the presence of DUI in bivalves has been related to the maintenance of gonochorism [78]. More data relating the presence of two Bbs to hermaphroditism in Bivalvia are needed to investigate this hypothesis.

The Cb observed in *R. philippinarum* early spermatids (Figure 3) is morphologically identical to those described in mouse [20,25] and rat [22,23,79]. It is always located close to the nuclear membrane and surrounded by empty mitochondria, some showing extruded cristae (Figure 3D), indicating their involvement in *R. philippinarum* Cb formation, as seen in sea urchins [33]. In the same cytoplasmic area, ribosomes with two different sizes and forming polyribosomes were found (Figure 3A–C), as reported for *Drosophila* [32]. Amikura et al. [35] demonstrated, by inhibition of prokaryotic-type translation, that the small ribosomes are of mitochondrial origin. The structural similarity between clams and model organisms suggests that these mitochondrial ribosomes play a similar role in the germ line development of this bivalve. In *R. philippinarum* spermatids, also the nucleus contributes to Cb formation, since material outflow from pores of the nuclear membrane can be seen in Cb proximity (Figure 3A–C), as documented in rats [79] and amphibians [80].

Vasph and germ line formation

To detect Vasa expression, we used an antibody against Vasa chicken (anti-Cvh) [72]. This antibody reacted in monodimensional immunoblotting of gonadic and embryonic extracts with a band of about 65 kDa (Figure 4A) that with bidimensional immunoblotting is resolved in three spots (Figure 4B), probably isoforms of the same protein, with mass and isoelectric point in the range of the known Vasa-homologs [14]. Further, we compared the sequence of *R. philippinarum* Vasa (Vasph) to chicken Vasa. The detection of one protein by western blot, the high CORE index of the alignment of Vasph and chicken Vasa-homolog (score = 95) (Figure 5) and the identification in Vasph of Vasa conserved domains by InterProScan (Figure 6) support the specific staining of the antibody used, even more considering the specific labeling observed in gametogenetic cells, while no staining was found in other tissues (intestine and connective) (Figure 7). Thus, Vasa appears to be a specific marker of germ cells in *R. philippinarum*, as in other animals (see [12–15,81–85]). Up to now, only the distribution of *vasa* mRNAs was analyzed in molluscs [86–91], and this is the first study about the immunolocalization of Vasa protein. Clam gonad is not permanent and the mechanism of its reformation every mating season is not fully documented. We showed that the wall of the acini are formed by Vasa labeled cells (germ cells). This cell aggregation defines an empty area in the middle (Figure 7C–F), the acinus lumen, which in mature gonads is full of gametes (Figure 7G and H).

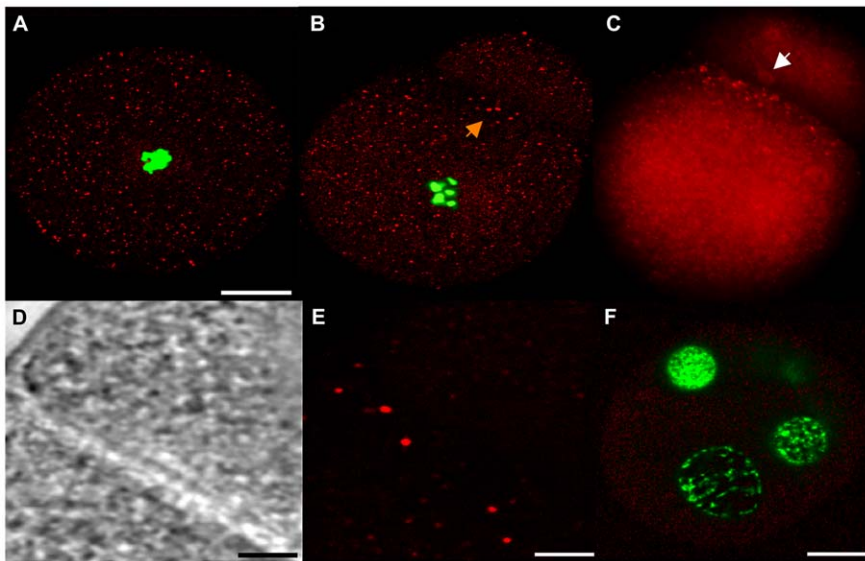


Figure 8. Vasph immunolocalization with anti-Cvh in *R. philippinarum* embryos. (A) Stained egg at confocal microscope showing small granules equally dispersed in the cytoplasm (20 μ m bar). (B) Confocal microscope analysis of a 2-blastomere embryo: some small stained spots are dispersed in the cytoplasm, but an aggregation of bigger granules with a stronger labeling is localized close to the cleavage furrow (arrow). Anti-Cvh and TO-PRO-3 iodide staining DNA are represented by red and green, respectively. (C) The same embryo under fluorescence microscope; a trace of the midbody can be perceived (white arrow) (B, C: same magnification of A). (D, E) The same detail of the cleavage shown in B, with transmitted light (D) and confocal microscope (E) (D, E: 4 μ m bar). (F) Confocal microscope analysis of a 4-blastomere embryo, in which only secondary antibody was used. No staining is visible (20 μ m bar).
doi:10.1371/journal.pone.0028194.g008

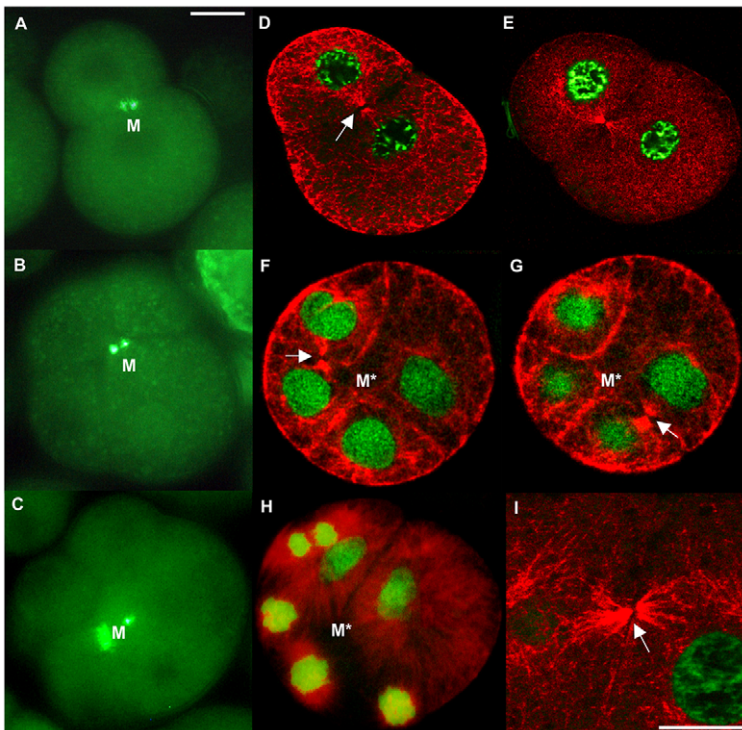


Figure 9. Distribution patterns of spermatozoon mitochondria and microtubules in *R. philippinarum* male early embryos. (A–C) Fluorescence microscope analysis. The staining with MitoTracker Green shows an aggregation of spermatozoon mitochondria (M, in light green) in 2- (A), 4- (B) and 8- (C) blastomere male embryos. (D–I) Confocal microscope analysis. (D, E) Microtubule immunolocalization in 2-blastomere male embryos. Anti- α -tubulin (red) and TO-PRO-3 iodide staining DNA (green). A well defined midbody (white arrow) is localized in the middle of the first cleavage furrow, corresponding to the area in which the four spermatozoon mitochondria aggregate in male embryos. (F, G) Microtubule immunolocalization in 4-blastomere male embryos. The two images are acquired at various depths within the same embryo: the two new spindles to form the 4-blastomere embryo are positioned in tangential directions, far from the region (M*) where the four M-type mitochondria localize (white arrows indicate the midbodies), as clearly shown also in 8-blastomere embryos (H) (bar 20 μ m). (I) Detail of a midbody (white arrow) (bar 15 μ m).
doi:10.1371/journal.pone.0028194.g009

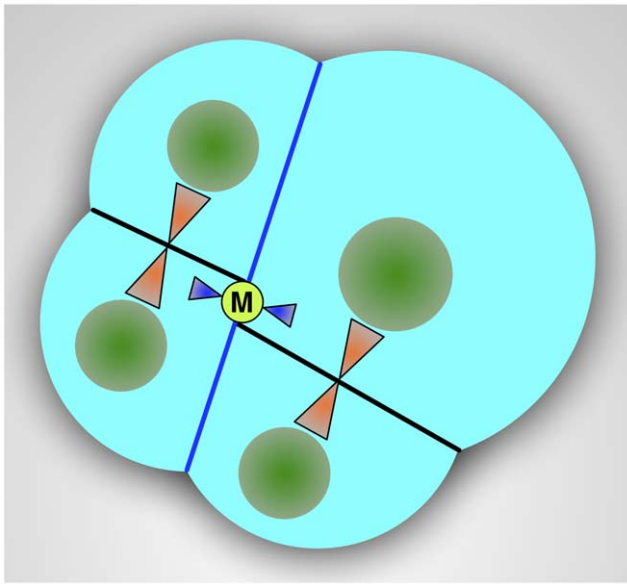


Figure 10. Segregation scheme of spermatozoon mitochondria in DUI male embryos. The scheme shows the position of the two midbodies (orange triangles) in a developing 4-blastomere embryo. The plane of the first cleavage is shown with a blue line, and the first midbody, by this time disassembled, is in blue. During the following divisions the same architecture is maintained, with the new spindles (orange) in tangential directions, far from the animal-vegetal axis on which spermatozoon mitochondria (M) were arranged (light green circle). Nuclei in dark green.
doi:10.1371/journal.pone.0028194.g010

Vasa is an evolutionary conserved component of the germ plasm [12–19], so we used this molecular marker to localize germ plasm both in eggs and in early embryos of *R. philippinarum*. In eggs labeled with anti-Cvh, a spotted staining dispersed in the cytoplasm was found, while a more strongly labeled zone was visible along the cleavage furrow in 2-blastomere embryos (Figure 8). This finding is in line with what found in embryos of other animals, in which Vasa localized in the middle portion of the first cleavage furrow [72]. This early Vasa segregation supports a preformation mechanism for germ line determination in *R. philippinarum*. In animals, germ cells can be specified by maternally inherited determinants (preformation) and by inductive signals from surrounding tissues during development (epigenesis) [92].

Among bivalves, in *Crassostrea gigas* [87] and *Sphaerium striatinum* [93] vasa mRNA is restricted to a defined zone during the first embryo stages suggesting a specification by preformation. The early segregation of Vasa in *R. philippinarum* suggests that maternal factors already present in the eggs could be involved in PGCs formation, supporting the hypothesis that maternal nuclear genes act as germ line determining factors (see also [68]).

Spermatozoon mitochondria and male germ line formation

As discussed, both nuclear and mitochondrial factors play a role in nuage formation in both SMI and DUI species. However, a few questions remain open in DUI species. How do sperm mitochondria enter male germ line? How do they displace the maternal mitochondria in the germ cells? In *M. galloprovincialis* sperm mitochondria and nucleus remain at the entry point of eggs treated with colchicine [49], suggesting a role of microtubules in the movements of sperm mitochondria soon after fertilization. In *R. philippinarum* embryos, the microtubule immunostaining showed a well-defined midbody in the middle of the first cleavage furrow, corresponding to the area in which the aggregate of spermatozoon mitochondria localizes (Figure 9). It is known that when the cleavage furrow ingresses compressing the spindle midzone, it creates an intercellular bridge containing a midbody at the center [94–96]. Thus, the midbody is a structure of tightly packed microtubules and associated proteins derived from the constriction of the central spindle [96]. Although no clear function has been ascribed to the midbody yet, it contains proteins indispensable for cytokinesis, asymmetric cell division, and chromosome segregation [95–97]. It might be also involved in the trafficking of important signaling molecules along the microtubules and in the segregation of material for germ line development. Indeed, the germ plasm is segregated into germ cells by dynein- and kinesin-dependent transport on centrosome-nucleated microtubules [8,98], and the disruption of some midbody proteins causes a failure in progeny production [95,99–101]. In this way, in many animals germ line determinants aggregate in the middle of the first cleavage furrow [72,102], where in DUI male embryos the aggregate of spermatozoon mitochondria localizes. In this context, M-type mitochondria may be recognized by specific motor proteins that would carry them to the central spindle, where the cleavage furrow of the 2-cell stage forms. The midbody appears to have a role in positioning M-type mitochondria in a stable zygote area on the a-v axis, avoiding a complete dispersal in the blastomeres: in spiral segmentation this central zone is not directly involved in the

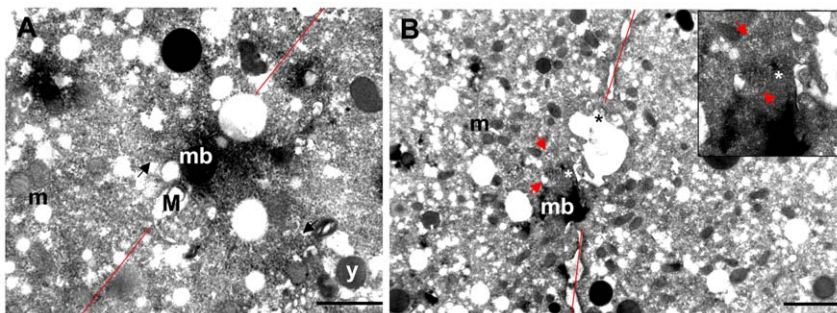


Figure 11. Ultrastructural analysis of *R. philippinarum* male early embryos. (A, B) 2-blastomere embryos showing a midbody (mb). The cleavage plane is marked with a red line. (A) One spermatozoon mitochondrion of about 1 μ m (M) is positioned near the midbody; black arrows indicate microtubules; m – egg mitochondria; y – yolk (bar 1 μ m). (B) The egg mitochondria (m), abundant at the cleavage level, are recognizable by the smaller size; some are fusing with the cleavage membrane (black asterisk). Spermatozoon mitochondria (red arrows) are visible near the midbody (mb); a centriole (white asterisk) appears to still link the sperm mitochondria (detail in the inset) (bar 2 μ m).
doi:10.1371/journal.pone.0028194.g011

cleavages, which take place around it [103], so that the mitochondrial aggregation can be maintained. As clearly shown in 4-blastomere embryos of *R. philippinarum*, the new spindles form in tangential directions, far from the region on the a-v axis where the aggregate of M-type mitochondria is located (Figures 9 and 10). Although microtubules emanate from the spindle poles during early anaphase, the microtubules of the central spindle eventually lose their connections with poles [104], and any material localized in the midzone can be easily maintained in position. TEM observations on sections of *R. philippinarum* 2-blastomere embryos showed F-type mitochondria at the division plane, some fused with the cleavage membrane (Figure 11), supporting their involvement in its building, as already proposed [95,105] and references therein). Moreover, the same sections showed a midbody in proximity of one or more mitochondria of about 1 μm in diameter (Figure 11). These should be interpreted as spermatozoon mitochondria, since no organelle of a comparable size was found in unfertilized oocytes. In some sections a complete spermatozoon midpiece was detected and a centriole appeared to still link the M-type mitochondria (Figure 11B). On the basis of our observations, in male embryos of *R. philippinarum* sperm mitochondria are not detached from the distal centriole of the midpiece, allowing simple transport to the midzone by microtubule nucleation. In mammals, the sperm mitochondrial sheath appears to be associated with microtubule-based structures to secure the destruction of sperm mitochondria in a specific compartment of the embryo [106]. In DUI species a similar mechanism could be responsible for the transportation of male mitochondria towards PGCs.

Recent studies have addressed the question about which mitochondria enter the germ line, i.e. whether they are a random

sub-sample or a selected small group, supporting the presence of a specific group of mitochondria in the germ plasm and their origin from the Bb [7,10,21,34]. This condition appears to be a conserved feature in SMI animals. However, it is unclear how these mitochondria are selected among the mitochondrial population of the egg. Some papers suggested they could be the healthiest mitochondria for a better embryo development [10,21,47,107,108]. In DUI species two types of mitochondria with highly divergent genomes are differently transmitted, indicating that only genomes with specific features must selectively enter the germ line [63,64]. During the development of DUI male embryos, spermatozoon mitochondria must be recognized by egg factors to be actively transferred by microtubules together with germ plasm in the PGCs, where they become dominant and replace Bb mitochondria during germ line formation.

Acknowledgments

We thank Prof. Franca Scanabissi, Adriana Paganini-Paganelli, and Catia Orrico for their precious help in TEM samples preparation set up, and Julia Saltz for language revision and comments on the manuscript.

Author Contributions

Conceived and designed the experiments: LM MP. Performed the experiments: LM MGM. Analyzed the data: LM. Contributed reagents/materials/analysis tools: MGM MP. Wrote the paper: LM FG. Discussed the data, commented on the manuscript drafts and approved the final manuscript: LM FG MGM MP.

References

- Eddy EM (1975) Germ plasm and the differentiation of the germ cell line. *Int Rev Cytol* 43: 229–281.
- Illmensee K, Mahowald AP, Loomis MR (1976) The ontogeny of germ plasm during oogenesis in *Drosophila*. *Dev Biol* 49: 40–65.
- Rongo C, Lehmann R (1996) Regulated synthesis, transport and assembly of the *Drosophila* germ plasm. *Trends Genet* 12: 102–109.
- Ikenishi K (1998) Germ Plasm in *Caenorhabditis elegans*, *Drosophila* and *Xenopus*. *Develop. Growth Differ* 40: 1–10.
- Saffman EE, Lasko P (1999) Germline development in vertebrates and invertebrates. *Cell Mol Life Sci* 55: 1141–1163.
- Wylie C (1999) Germ cells. *Cell* 96: 165–174.
- Matova N, Cooley L (2001) Comparative Aspects of Animal Oogenesis. *Dev Biol* 231: 291–320.
- Becalska AN, Gavis EG (2010) Bazooka regulates microtubule organization and spatial restriction of germ plasm assembly in the *Drosophila* oocyte. *Dev Biol* 340: 528–538.
- Kloc M, Bilinski S, Chan AP, Allen LH, Zearfoss NR, et al. (2001) RNA localization and germ cell determination in *Xenopus*. *Int Rev Cytol* 203: 63–91.
- Kloc M, Bilinski S, Etkin LD (2004) The Balbiani body and germ cell determinants: 150 years later. *Curr Top Dev Biol* 59: 1–36.
- Kloc M, Etkin LD (2005) RNA localization mechanisms in oocytes. *J Cell Sci* 118: 269–282.
- Hay B, Ackerman L, Barbel S, Jan LY, Jan YN (1988) Identification of a component of *Drosophila* polar granules. *Development* 103: 625–640.
- Hay B, Jan LY, Jan YN (1988) A protein component of *Drosophila* polar granules is encoded by vasa and has extensive sequence similarity to ATP-dependent helicases. *Cell* 55: 577–587.
- Gustafson EA, Wessel GM (2010) Vasa genes: emerging roles in the germ line and in multipotent cells. *Bioessays* 32: 626–637.
- Lasko F, Ashburner M (1988) The product of the *Drosophila* gene vasa is very similar to eucaryotic initiation factor-4A. *Nature* 335: 611–617.
- Williamson A, Lehmann R (1996) Germ Cell Development in *Drosophila*. *Annu Rev Devel Biol* 12: 365–391.
- Knaut H, Pelegri F, Bohmann K, Schwarz H, Nusslein-Volhard C (2000) Zebrafish vasa RNA but not its protein is a component of the germ plasm and segregates asymmetrically before germline specification. *J Cell Biol* 149: 875–888.
- Kuznicki KA, Smith PA, Leung-Chiu WM, Estevez AO, Scott HC, et al. (2000) Combinatorial RNA interference indicates GLH-4 can compensate for GLH-1; these two P granule components are critical for fertility in *C. elegans*. *Development* 127: 2907–2916.
- Raz E (2000) The function and regulation of vasa-like genes in germ-cell development. *Genome Biol* 1: REVIEWS1017.1–1017.6.
- Reunov A (2006) Structures related to the germ plasm in mouse. *Zygote* 14: 231–238.
- Cox RT, Spradling AC (2003) A Balbiani body and the fusome mediate mitochondrial inheritance during *Drosophila* oogenesis. *Development* 130: 1579–1590.
- Russell L, Frank B (1978) Ultrastructural characterization of nuage in spermatocytes of the rat testis. *Anat Rec* 190: 79–97.
- Parvinen M (2005) The chromatoid body in spermatogenesis. *Int J Androl* 28: 189–201.
- Kotaja N, Bhattacharyya SN, Jaskiewicz L, Kimmins S, Parvinen M, et al. (2006) The chromatoid body of male germ cells: Similarity with processing bodies and presence of Dicer and microRNA pathway components. *Proc Natl Acad Sci U S A* 103: 2647–2652.
- Kotaja N, Sassone-Corsi P (2007) The chromatoid body: a germ-cell-specific RNA-processing centre. *Nat Rev Mol Cell Bio* 8: 85–90.
- Shang P, Baarends WM, Hoogerbrugge J, Ooms MP, van Cappellen WA, et al. (2010) Functional transformation of the chromatoid body in mouse spermatids requires testis-specific serine/threonine kinases. *J Cell Sci* 123: 331–339.
- Kobayashi S, Amikura R, Okada M (1993) Presence of Mitochondrial Large Ribosomal RNA Outside Mitochondria in Germ Plasm of *Drosophila melanogaster*. *Science* 260: 1521–1524.
- Ding D, Whittaker KL, Lipshitz HD (1994) Mitochondrially Encoded 16S Large Ribosomal RNA is Concentrated in the Posterior Polar Plasm of Early *Drosophila* Embryos but is not Required for Pole Cell Formation. *Dev Biol* 163: 503–515.
- Iida T, Kobayashi S (1998) Essential role of mitochondrially encoded large rRNA for germ-line formation in *Drosophila* embryos. *Proc Natl Acad Sci U S A* 95: 11274–11278.
- Kobayashi S, Amikura R, Mukai M (1998) Localization of Mitochondrial RNA in Germ Plasm of *Xenopus* Embryos. *Curr Biol* 8: 1117–1120.
- Ogawa M, Amikura R, Akasaka K, Kinoshita T, Kobayashi S, et al. (1999) Asymmetrical Distribution of Mitochondrial rRNA into Small Micromeres of Sea Urchin Embryos. *Zool Sci* 16: 445–451.
- Amikura R, Kashikawa, M, Nakamura A, Kobayashi S (2001) Presence of mitochondria-type ribosomes outside mitochondria in germ plasm of *Drosophila* embryos. *Proc Natl Acad Sci U S A* 98: 9133–9138.
- Reunov A, Isaeva V, Au D, Wu R (2000) Nuage constituents arising from mitochondria: Is it possible? *Develop Growth Differ* 42: 139–143.

34. Isaeva VV, Reunov AA (2001) Germ Plasm and Germ-line Cell Determination: The Role of Mitochondria. *Russ J Mar Biol* 27: S8–S14.
35. Amikura R, Sato K, Kobayashi S (2005) Role of mitochondrial ribosome-dependent translation in germline formation in *Drosophila* embryos. *Mech Develop* 122: 1087–1093.
36. Andersson SGE, Zomorodipour A, Andersson JO, Sicheritz-Pontén T, Alsmark UCM, et al. (1998) The genome sequence of *Rickettsia prowazekii* and the origin of Mitochondria. *Nature* 396: 133–143.
37. Ebbert MA (1993) Endosymbiotic sex ratio distorters in insects and mites. In: Wrensh DL, Ebbert MA, eds. *Evolution and Diversity of Sex Ratio in Insects and Mites*. New York: Chapman Hall. pp 150–191.
38. Hurst GDD, Hurst LD, Majerus MEN (1997) Cytoplasmic sex-ratio distorters. In: O'Neil SL, Hoffmann AA, Werren JH, eds. *Influential Passengers: Inherited Microorganisms and Invertebrate Reproduction*. UK: Oxford University Press. pp 125–154.
39. Negri I, Franchini A, Gonella E, Daffonchio D, Mazzoglio PJ, et al. (2009) Unravelling the *Wolbachia* evolutionary role: the reprogramming of the host genomic imprinting. *Proc R Soc B* 276: 2485–2491.
40. Smiraglia DJ, Kulawiec M, Bistulfi GL, Gupta SG, Singh KK (2008) A novel role for mitochondria in regulating epigenetic modification in the nucleus. *Cancer Biol Ther* 7: 1182–1190.
41. Cao L, Shitara H, Horii T, Nagao Y, Imai H, et al. (2007) The mitochondrial bottleneck occurs without reduction of mtDNA content in female mouse germ cells. *Nat Genet* 39: 386–390.
42. Shoubridge EA, Wai T (2007) Mitochondrial DNA and the mammalian oocyte. *Curr Top Dev Biol* 77: 87–111.
43. Cree LM, Samuels DC, de Sousa Lopes SC, Rajasimha HK, Wonnapijit P, et al. (2008) A reduction of mitochondrial DNA molecules during embryogenesis explains the rapid segregation of genotypes. *Nat Genet* 40: 249–254.
44. Tourte M, Mignotte F, Mounolou JC (1984) Heterogeneous distribution and replication activity of mitochondria in *Xenopus laevis* oocytes. *Eur J Cell Biol* 34: 171–178.
45. Mignotte F, Tourte M, Mounolou JC (1987) Segregation of mitochondria in the cytoplasm of *Xenopus* vitellogenic oocytes. *Cell* 60: 97–102.
46. Volodina N, Denegre JM, Mowry KL (2003) Apparent Mitochondrial Asymmetry in *Xenopus* Eggs. *Dev Dynam* 226: 654–662.
47. Zhou RR, Wang B, Wang J, Schatten H, Zhang YZ (2010) Is the mitochondrial cloud the selection machinery for preferentially transmitting wild-type mtDNA between generations? Rewinding Müller's ratchet efficiently. *Curr Genet* 56: 101–107.
48. Chuma S, Hosokawa M, Tanaka T, Nakatsuji N (2009) Ultrastructural characterization of spermatogenesis and its evolutionary conservation in the germline: germinal granules in mammals. *Mol Cell Endocrinol* 306: 17–23.
49. Obata M, Komaru A (2005) Specific location of sperm mitochondria in mussel *Mytilus galloprovincialis* zygotes stained by MitoTracker. *Dev Growth Differ* 47: 255–263.
50. Katayama M, Zhong Z, Lai L, Sutovsky P, Prather RS, et al. (2006) Mitochondrial distribution and microtubule organization in fertilized and cloned porcine embryos: Implications for developmental potential. *Dev Biol* 299: 206–220.
51. Zhang YZ, Ouyang YC, Hou Y, Schatten H, Chen DY, et al. (2008) Mitochondrial behavior during oogenesis in zebrafish: A confocal microscopy analysis. *Develop Growth Differ* 50: 189–201.
52. Breton S, Beaupré HD, Stewart DT, Hoch WR, Blier PU (2007) The unusual system of doubly uniparental inheritance of mtDNA: isn't one enough? *Trends Genet* 23: 465–474.
53. Passamonti M, Ghiselli F (2009) Doubly Uniparental Inheritance: Two Mitochondrial Genomes, One Precious Model for Organelle DNA Inheritance and Evolution. (Review). *DNA Cell Biol* 28: 79–89.
54. Kaneda H, Hayashi J, Takahama S, Taya C, Fischer Lindhal K, et al. (1995) Elimination of paternal mitochondrial DNA in intraspecific crosses during early mouse embryogenesis. *Proc Natl Acad Sci U S A* 92: 4542–4546.
55. Shitara H, Hayashi JI, Takahama S, Kaneda H, Yonekawa H (1998) Maternal inheritance of mouse mtDNA in interspecific hybrids: segregation of the leaked paternal mtDNA followed by the prevention of subsequent paternal leakage. *Genetics* 148: 851–857.
56. Sutovsky P, Moreno RD, Ramalho-Santos J, Dominko T, Simerly C, et al. (1999) Ubiquitin tag for sperm mitochondria. *Nature* 402: 371–372.
57. Sutovsky P, Moreno RD, Ramalho-Santos J, Dominko T, Simerly C, et al. (2000) Ubiquitinated sperm mitochondria, selective proteolysis, and the regulation of mitochondrial inheritance in mammalian embryos. *Biol Reprod* 63: 582–590.
58. Theologidis I, Fodelianakis S, Gaspar MB, Zouros E (2008) Doubly uniparental inheritance (DUI) of mitochondrial DNA in *Donax trunculus* (Bivalvia: Donacidae) and the problem of its sporadic detection in Bivalvia. *Evol Int J Org Evol* 62: 959–970.
59. Doucet-Beaupré H, Breton S, Chapman EG, Blier PU, Bogan AE, et al. (2010) Mitochondrial phylogenomics of the Bivalvia (Mollusca): Searching for the origin and mitogenomic correlates of doubly uniparental inheritance of mtDNA. *BMC Evol Biol* 10: 50.
60. Cao L, Kenchington E, Zouros E (2004) Differential segregation patterns of sperm mitochondria in embryos of the blue mussel (*Mytilus edulis*). *Genetics* 166: 883–894.
61. Cogswell AT, Kenchington ELR, Zouros E (2006) Segregation of sperm mitochondria in two- and four-cell embryos of the blue mussel *Mytilus edulis*: implications for the mechanism of doubly uniparental inheritance of mitochondrial DNA. *Genome* 49: 799–807.
62. Milani L, Ghiselli F, Passamonti M. Sex-linked mitochondrial behavior during early embryo development in Ruditapes philippinarum (Bivalvia Veneridae) a species with the Doubly Uniparental Inheritance (DUI) of mitochondria. *J Exp Zool Part B*, in press.
63. Venetis C, Theologidis I, Zouros E, Rodakis GC (2006) No evidence for presence of maternal mitochondrial DNA in the sperm of *Mytilus galloprovincialis* males. *Proc Biol Sci* 273: 2483–2489.
64. Ghiselli F, Milani L, Passamonti M (2011) Strict sex-specific mtDNA segregation in the germline of the DUI species *Venerupis philippinarum* (Bivalvia Veneridae). *Mol Biol Evol* 28: 949–961.
65. Saavedra C, Reyero MI, Zouros E (1997) Male-dependent doubly uniparental inheritance of mitochondrial DNA and female-dependent sex-ratio in the mussel *Mytilus galloprovincialis*. *Genetics* 145: 1073–1082.
66. Sutherland B, Stewart DT, Kenchington E, Zouros E (1998) The fate of paternal mitochondrial DNA in developing female mussels, *Mytilus edulis*: implications for the mechanism of doubly uniparental inheritance of mitochondrial DNA. *Genetics* 148: 341–347.
67. Kenchington E, MacDonald B, Cao L, Tsagkarakis D, Zouros E (2002) Genetics of mother-dependent sex ratio in blue mussels (*Mytilus* spp.) and implications for doubly uniparental inheritance of mitochondrial DNA. *Genetics* 161: 1579–1588.
68. Ghiselli F, Milani L, Chang PL, Hedgecock D, Davis JP, Nuzhdin SV, Passamonti M (2011) *De Novo* Assembly of the Manila clam *Ruditapes philippinarum* Transcriptome Provides New Insights into Expression Bias, Mitochondrial Doubly Uniparental Inheritance and Sex Determination. *Mol Biol Evol*; doi: 10.1093/molbev/msr248.
69. Devauchelle N (1990) Sexual development and maturity of *Tapes philippinarum*. In: *Tapes philippinarum*, biologia e sperimentazione. Ente Sviluppo Agricolo Veneto (ESAV), chapter 3.
70. Hejnal A (2010) A Twist in Time—The Evolution of Spiral Cleavage in the Light of Animal Phylogeny. *Integr Comp Biol* 50: 695–706.
71. Laemmli UK (1970) Cleavage of structural proteins during the assembly of the head of bacteriophage T4. *Nature* 227: 680–685.
72. Tsunekawa N, Naito M, Sakai Y, Nishida T, Noce T (2000) Isolation of chicken vasa homolog gene and tracing the origin of primordial germ cells. *Development* 127: 2741–2750.
73. Maurizii MG, Cavaliere V, Gamberi C, Lasko P, Gargiulo G, et al. (2009) Vasa protein is localized in the germ cells and in the oocyte-associated pyroform follicle cells during early oogenesis in the lizard *Podarcis sicula*. *Dev Genes Evol* DOI 10.1007/s00427-009-0295-7.
74. Notredame C, Higgins DG, Heringa J (2000) T-Coffee: A novel method for fast and accurate multiple sequence alignment. *J Mol Biol* 302: 205–217.
75. Hunter S, Apweiler R, Attwood TK, Bairoch A, Bateman A, et al. (2009) InterPro: the integrative protein signature database. *Nucleic Acids Res* 37(Database Issue): D211–D215.
76. Notredame C, Abergel C (2003) Using T-Coffee to assess the reliability of multiple sequence alignments. In: Andrade MA, ed. *Bioinformatics and Genomes*. Wymondham, UK: Horizon Scientific Press. pp 27–49.
77. Davison A (2006) The ovotestis: an underdeveloped organ of evolution. *BioEssays* 28: 642–650.
78. Breton S, Stewart DT, Shepardson S, Trdan RJ, Bogan AE, et al. (2011) Novel Protein Genes in Animal mtDNA: A New Sex Determination System in Freshwater Mussels (Bivalvia: Unionoida)? *Mol Biol Evol* 28: 1645–1659.
79. Söderström KO, Parvinen M (1976) Transport of material between the nucleus, the chromatoid body and the Golgi complex in the early spermatids of the rat. *Cell Tissue Res* 168: 335–342.
80. Peruquetti RL, Taboga SR, de Souza Santos LR, de Oliveira C, de Azeredo-Oliveira MTV (2011) Nucleolar cycle and chromatoid body formation: Is there a relationship between these two processes during spermatogenesis of *Dendropsophus minutus* (Amphibia, Anura)? *Micron* 42: 87–96.
81. Komiya T, Itoh K, Ikenishi K, Furusawa M (1994) Isolation and characterization of a novel gene of the DEAD Box protein family which is specifically expressed in germ cell of *Xenopus laevis*. *Dev Biol* 162: 354–363.
82. Nakao H (1999) Isolation and characterization of a *Bombyx* vasa-like gene. *Dev Genes Evol* 209: 316–321.
83. Castrillon DH, Quade BJ, Wang TY, Quigley C, Crum CP (2000) The human VASA gene is specifically expressed in the germ cell lineage. *Proc Natl Acad Sci U S A* 97: 9585–9590.
84. Kobayashi T, Kajiura-Kobayashi H, Nagahama Y (2000) Differential expression of vasa homologue gene in the germ cells during oogenesis and spermatogenesis in a teleost fish, tilapia, *Oreochromis niloticus*. *Mech Dev* 99: 139–142.
85. Mochizuki K, Nishimiya-Fujisawa C, Fujisawa T (2001) Universal occurrence of the vasa-related genes among metazoans and their germline expression in *Hydra*. *Dev Genes Evol* 211: 299–308.
86. Fabioux C, Pouvreau S, Le Roux F, Huvet A (2004) The oyster vasa-like gene: a specific marker of the germline in *Crassostrea gigas*. *Biochem Biophys Res Commun* 315: 897–904.

87. Fabioux C, Huvet A, Lelong C, Robert R, Pouvreau S, et al. (2004) Oyster vasa-like gene as a marker of the germline cell development in *Crassostrea gigas*. *Biochem Biophys Res Commun* 320: 592–598.
88. Kakoi S, Kin K, Miyazaki K, Wada H (2008) Early Development of the Japanese Spiny Oyster (*Saccostrea kegakû*): Characterization of Some Genetic Markers. *Zool Sci* 25: 455–464.
89. Swartz SZ, Chan XY, Lambert JD (2008) Localization of Vasa mRNA during early cleavage of the snail *Ilyanassa*. *Dev Genes Evol* 218: 107–113.
90. Kranz AM, Tollenaere A, Norris BJ, Degnan BM, Degnan SM (2010) Identifying the Germline in an Equally Cleaving Mollusc: *Vasa* and *Nanos* Expression During Embryonic and Larval Development of the Vetigastropod *Haliotis asinina*. *J Exp Zool Part B* 314: 1–13.
91. Obata M, Sano N, Kimata S, Nagasawa K, Yoshizaki G, Komaru A (2010) The proliferation and migration of immature germ cells in the mussel, *Mytilus galloprovincialis*: observation of the expression pattern in the *M. galloprovincialis* vasa-like gene (*Myvlg*) by in situ hybridization. *Dev Genes Evol* 220: 139–149.
92. Extavour CG, Akam M (2003) Mechanisms of germ cell specification across the metazoans: epigenesis and preformation. *Development* 130: 5869–5884.
93. Woods FH (1931) History of the germ cells in *Sphaerium striatinum* (Lam.). *J Morphol* 51: 545–595.
94. Pawelczak N (2001) Walther Flemming: pioneer of mitosis research. *Nature Rev Mol Cell Biol* 2: 72–75.
95. Skop AR, Liu H, Yates J, III, Meyer BJ, Heald R (2004) Dissection of the Mammalian Midbody Proteome Reveals Conserved Cytokinesis Mechanisms. *Science* 305: 61–66.
96. Eggert US, Mitchison TJ, Field CM (2006) Animal Cytokinesis: From Parts List to Mechanisms. *Annu Rev Biochem* 75: 543–66.
97. Cai S, Weaver LN, Ems-McClung SC, Walczak CE (2010) Proper Organization of Microtubule Minus Ends Is Needed for Midzone Stability and Cytokinesis. *Curr Biol* 20: 880–885.
98. Lerit DA, Gavis ER (2011) Transport of Germ Plasm on Astral Microtubules Directs Germ Cell Development in *Drosophila*. *Curr Biol* 21: 439–448.
99. Gönczy P, Echeverri G, Oegema K, Coulson A, Jones SJ, et al. (2000) Functional genomic analysis of cell division in *C. elegans* using RNAi of genes on chromosome III. *Nature* 408: 331–336.
100. Piano F, Schetter AJ, Mangone M, Stein L, Kempthorn KJ (2000) RNAi analysis of genes expressed in the ovary of *Caenorhabditis elegans*. *Curr Biol* 10: 1619–1622.
101. Maeda I, Kohara Y, Yamamoto M, Sugimoto A (2001) Large-scale analysis of gene function in *Caenorhabditis elegans* by high-throughput RNAi. *Curr Biol* 11: 171–176.
102. Kloc M, Larabell C, Chan AP, Etkin LD (1998) Contribution of METRO pathway localized molecules to the organization of the germ cell lineage. *Mech Dev* 75: 81–93.
103. Tyler SEB, Kimber SJ (2006) The dynamic nature of mollusc egg surface architecture and its relation to the microtubule network. *Int J Dev Biol* 50: 405–412.
104. Glotzer M (2009) The 3Ms of central spindle assembly: microtubules, motors and MAPs. *Nat Rev Mol Cell Biol* 10: 9–20.
105. Bieliavsky N, Geuskens M (1990) Interblastomeric plasma membrane formation during cleavage of *Xenopus laevis* embryos. *J Submicrosc Cytol Pathol* 22: 445–57.
106. Sutoy P, Navara CS, Schatten G (1996) Fate of the Sperm Mitochondria, and the Incorporation, Conversion, and Disassembly of the Sperm Tail Structures during Bovine Fertilization. *Biol Reprod* 55: 1195–1205.
107. Boldogh IR, Pon LA (2006) Interactions of mitochondria with the actin cytoskeleton. *Biochimica et Biophysica Acta* 1763: 450–462.
108. Kogo N, Tazaki A, Kashino Y, Morichika K, Orii H, Mochii M, Watanabe K (2011) Germ-line mitochondria exhibit suppressed respiratory activity to support their accurate transmission to the next generation. *Dev Biol* 349: 462–469.